Low energy large scan field electron beam column for wafer inspection

X. Liu,[a] X. Zhang, Y. Zhao, A. Desai, and Z. W. Chen
Hermes Microvision, Inc., 1595 McCandless Drive, Milpitas, California 95035

(Received 4 June 2004; accepted 12 October 2004; published 14 December 2004)

A swing objective retarding immersion lens (SORIL) column for wafer inspection is designed and constructed based on SOIL concept. The column consists of a compound retarding electrostatic and magnetic immersion lens and five electrostatic deflectors. The retarding electrostatic and magnetic immersion lens has small spherical and chromatic aberration coefficients for low landing energy. All electrostatic deflectors have a cylindrical duodecapole structure. One deflector is accommodated between the polepiece of the magnetic lens and the specimen surface, and operated at high voltage to fulfill SOIL condition. An on-axis annular semiconductor detector with a small opening in the center is employed to collect signal electrons. The annular detector achieves high collection efficiency over a large scan field. Experimental results show that the SORIL column has accomplished a 600 μm $\times$ 600 μm scan field with 0.1 μm maximum spot size in a wide landing energy range (from 200 to 2000 eV) without dynamic aberration correction or dynamic focusing. Resolution of 15 nm is achieved in a 50 μm $\times$ 50 μm scan field. The probe beam current delivered by the SORIL column is from a few nA to more than 100 nA because of the specially designed bright electron gun. The SORIL column has been installed onto HMI's electron beam wafer inspection tool, eScan™ 300. The SORIL's optical performances enable eScan™ 300 to be a powerful electron beam wafer inspection and in-line process monitoring tool. © *2004 American Vacuum Society.* [DOI: 10.1116/1.1827629]

I. INTRODUCTION

Since the scanning electron microscope (SEM) was introduced into the semiconductor industry as a wafer inspection tool,[1] the low energy SEM has become indispensable to the development of new wafer processing technology and the enhancement of production yield. As the semiconductor technology enters the sub-100 nm node, new requirements for the electron beam column arise: wider low landing energy range, higher resolution and larger scan field. On one hand, since low-*k* dielectrics and other new materials are being utilized in the wafer processing, charging of the wafer during electron beam scanning is almost inevitable. In order to minimize the charging effect, the primary beam energy needs to be at one of the crossover points of the total electron yield curve as a function of primary beam energy, where the total electron yield equals unity. The secondary electron yield of most materials (insulators as well as conductors) reaches its maximum with the primary beam energy between 100 and 2000 eV. Therefore the electron beam column should have the capability to operate from a few hundred to a few thousand eV. On the other hand, the shrinking of the small feature size of the integrated circuit technology down to 45 nm and even smaller requires that resolution of the electron beam column be better than 30 nm, so that it is still able to detect the defects which are smaller than 45 nm. This is already beyond the resolution ability of the optical microscopy. Another issue to deal with when employing the electron beam inspection tool into the production line is throughput, which ideally should be defined as wafers per hour, not the current hours per wafer. For electron beam column based on the scanning mode, inspection of 100% area of the wafer is impossible in 1 h. An alternative way to resolve the throughput issue is to use the sampling method such as whole wafer die sampling (WWDS), where selected areas within a die are inspected for all the dies. If the electron beam column can scan a large field, the throughput can be accordingly improved.

In response to these requirements for the electron beam column for wafer inspection, a swing objective retarding immersion lens (SORIL) electron optical column has been developed. The electron optical properties of the SORIL column include: a scan field of 600 μm $\times$ 600 μm, a landing energy range from 200 to 2000 eV, the spot size from 15 to 100 nm, and the probe current from a few nanoampere to more than 100 nanoampere. The design theory of the SORIL, the configuration of the column, some practical design considerations and the experimental results are described in this article.

II. GENERAL CONDITION FOR ELECTROSTATIC DEFLECTION SWING OBJECTIVE IMMERSION LENS

The main obstacles for achieving a large scan field for a compound focusing-deflection electron beam system are the off-axis deflection geometrical aberrations, such as coma, astigmatism and field curvature. The theory of moving objective lens (MOL) was proposed to minimize off-axis deflection aberrations.[2] Based on the MOL, improved concepts such as variable axis lens (VAL)[3] and swing objective lens (SOL)[4] were developed and implemented in some modern electron beam systems, such as VAIL[5] and SOIL system.[6] In

[a]Author to whom correspondence should be addressed; electronic mail: xuedong.liu@hermes-microvision.com

these systems, however, the objective lens and the deflectors are of the same field type; usually magnetic deflectors are employed to shift the axis of a magnetic objective lens. This is because the conditions of the deflection fields to achieve MOL, VAL and SOL were derived from the magnetic lens's field distribution expressed in the power series.[2–4] The method to accomplish MOL, VAL and SOL conditions for the electron optics system whose lens and deflectors have different field types is still under development.

The general conditions for the first-order MOL, VAL, and SOL can be derived based on the paraxial trajectory equation.[7,8] For a compound focusing-deflection system, the paraxial trajectory is described by the following equation:

$$w'' + \frac{\phi'}{2\phi}w' + \frac{\phi''}{4\phi}w - i\sqrt{\frac{\eta}{2\phi}}\left(Bw' - \frac{1}{2}B'w\right) = -\frac{VE_1}{2\phi} - i\sqrt{\frac{\eta}{2\phi}}ID_1, \tag{1}$$

where $w=x+iy$ denotes the paraxial trajectory, ϕ the axial potential, B the axial magnetic field, $\eta=e/m$ the electron charge-to-mass ratio, E_1 the electrostatic deflection field under unit deflection voltage, D_1 the magnetic deflection field under unit excitation current, $V=V_x+iV_y$ is the voltage applied to the x and y electrostatic deflector electrodes, and $I=I_x+iI_y$ is the excitation current applied to the x and y deflection coils. The initial conditions of the primary electron beam after pre-deflection can be expressed as

$$\begin{cases} w_0 = x_0 + iy_0 \\ w_0' = k_0 = x_0' + iy_0'. \end{cases} \tag{2}$$

If the primary electron beam enters the objective lens and passes the compound field of focusing and deflection without disturbance, the beam trajectory can be expressed by

$$w = w_0 + k_0(z - z_0) \quad (z_0 \leqslant z \leqslant z_i). \tag{3}$$

Of course Eq. (3) should be a solution of the paraxial trajectory equation (1) if the electron beam is not bent by the deflection field. Substituting Eq. (3) into Eq. (1), the relationship between the lens field and the deflection field can be derived as

$$k_0\frac{\phi'}{2\phi} + \frac{\phi''}{4\phi}[k_0(z - z_0) + w_0] - i\sqrt{\frac{\eta}{2\phi}}\left\{k_0B - \frac{1}{2}B'[k_0(z - z_0) + w_0]\right\} = -\frac{VE_1}{2\phi} - i\sqrt{\frac{\eta}{2\phi}}ID_1. \tag{4}$$

From this equation, the general condition of the MOL, VAL and SOL for any combination of lens and deflection field type can be obtained.[7,8]

If only electrostatic deflectors are applied to shift the axis of a compound electrostatic and magnetic lens, the SOL condition becomes

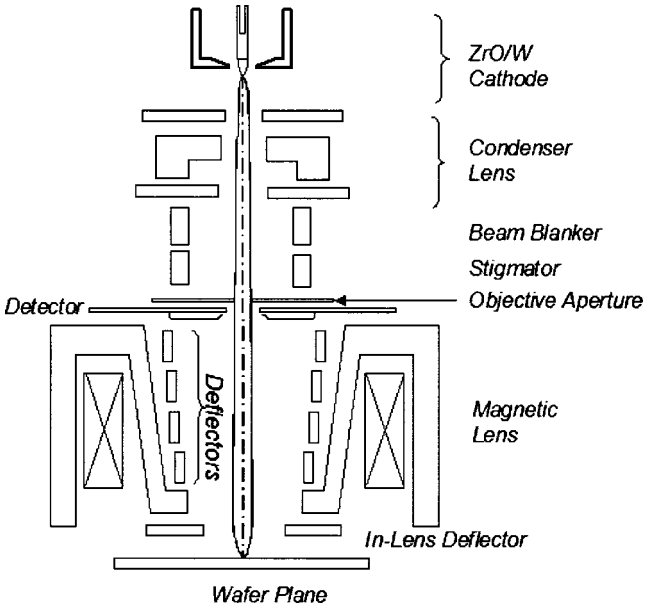

FIG. 1. Schematic drawing of the SORIL column.

$$-VE_1 = k_0\phi' + \frac{1}{2}k_0\phi''(z - z_0) - i\sqrt{2\phi\eta}\left[k_0B - \frac{1}{2}k_0B'(z - z_0)\right]. \tag{5}$$

Due to the nonlinear distribution of the electrostatic and magnetic lens field, an exact match of the deflection field and the lens field is very difficult to implement into a practice design. Equation (5) shows us that an electrostatic deflection field superimposed onto the objective lens field has the possibility of fulfilling the SOL condition even if a compound retarding electrostatic and magnetic immersion lens is adopted into a practical column design. After the axis of the compound lens is shifted and swung by the electrostatic deflection field, the off-axis aberrations of the focusing-deflection system are reduced greatly, and a large scan field becomes achievable.

III. DESCRIPTION OF THE SORIL COLUMN

A schematic of the SORIL column is shown in Fig. 1. The whole system consists of a thermal field emission source, an electrostatic condenser lens, a beam blanker, an astigmatism corrector, a compound electrostatic retarding and magnetic immersion objective lens, a deflection system and an on-axis annular electron detector. A detailed description of each component of the SORIL column and practical consideration are presented in the following sections.

A. Electron gun

A ZrO/W thermal field emission electron gun operated at 1800 K is designed and constructed to provide a point electron source. Electrons emitted from the ZrO/W cathode are accelerated to 12 kV. The accelerated electron beam is prefocused by an electrostatic condenser lens, followed by a

stigmator and a beam blanker. Special shield plates made of high magnetic permeability metal are designed to prevent impact of the stray magnetic field on the primary beam. Two ion pumps are used on the gun chamber, allowing differential pumping between its upper and lower sections, which maintains ultrahigh vacuum around the electron emitter. The beam exit on the gun chamber can be sealed from the outer environment by a gate valve, so that its inside vacuum can be always preserved for ease of transportation and system maintenance.

B. Objective lens

A compound retarding electrostatic and magnetic immersion lens is adopted as the objective lens because this lens is known to have excellent electron optical properties.[9] Except in the vicinity of the cathode and near the wafer surface, the electron beam moves at high speed along the path of the whole column. This makes the SORIL column tolerant to stray magnetic fields, and also greatly minimizes the impact of electron-electron interaction on the beam resolution.

The designed magnetic lens has a large size bore, with its polepiece opening facing the specimen, as the magnetic lens with large side pole gap has been proven to have very low aberration coefficients.[10] The specimen is positioned at the peak of the axial magnetic field distribution, which is far below the polepiece of the magnetic lens. A large movable stage is employed to hold the wafer. The fact that the specimen is immersed in a strong magnetic field is also very helpful in improving the collection efficiency of secondary electrons, especially for high aspect ratio structures. The long working distance between the polepiece and the specimen makes it possible to accommodate an in-lens deflector, which is crucial to achieving a large scan field. The large bore size of the polepiece makes a relative large paraxial zone along the radial direction, which is helpful in reducing the field curvature and achieving a large scan field without dynamic compensation or dynamic focusing. In addition, the requirements for the machining precision of the polepiece and the concentricity of the different components during assembling become less stringent.

C. Deflection system

Five electrostatic deflectors are used in the SORIL column to achieve a large scan field, as shown in Fig. 1. One pair of deflectors works as pre-lens double deflection system for subfield scan, and achieves a 50 μm $\times$ 50 μm scan field. The rest set of three deflectors scans a main field of 600 μm $\times$ 600 μm. Among the three main field deflectors, the top deflector is placed as far as possible from the objective lens and pre-deflects the electron beam. When entering the objective lens field region, the electron beam has a small slope but a large offset from the lens axis. The middle deflector shifts the electron beam further from the lens axis. The bottom in-lens deflector is sandwiched between the wafer surface and magnetic lens polepiece and is biased at high voltage. The deflection field of the in-lens deflector overlaps with the objective lens field and swings the axis of the compound objective lens by matching the SOL condition of Eq. (5).

Electrostatic deflectors are chosen for SORIL column because they can scan at a fast speed. On the contrary, magnetic deflectors suffer from the speed limitation due to the eddy current effect if it is positioned in the vicinity of the magnetic polepole. In addition, electrostatic deflectors can be designed to have compact size and accurate shape to fit the limited space in the vicinity of the magnetic objective lens and center well with the magnetic objective lens.

All five electrostatic deflectors have cylindrical duodecapole (12 pole) structure. In modern electron beam systems three typical cylindrical deflectors are utilized: octupole, duodecapole and icosapole (20 pole) structure. They have been investigated and analyzed in detail.[11,12] Theoretically the octupole and icosapole deflectors have better electron optical performances than the duodecapole because they can eliminate the third- and fifth-order harmonic multipole components when the gaps between subpoles and the applied potential are optimized. The duodecapole deflector is only free of third-order multipole component. But the octupole deflector needs eight independent electronic drivers. The structure of the icosapole deflector is too complicated. Some electrodes of the icosapole deflector are so small that it is very difficult to machine and assemble. The fifth and higher-order multipole harmonic terms of the deflection field contribute only to the fifth and high-order deflection aberrations, which are negligible compared with the third-order terms. So the duodecapole deflectors become our preferred choice for the SORIL column.

D. Detection of secondary and backscattered electrons

After secondary and backscattered electrons escape from the specimen surface, they are extracted and accelerated to a high energy over a very short distance by the strong electrostatic field over the specimen surface. At the same time the magnetic lens field collimates secondary electrons to the axis of the lens system. These signal electrons move in the opposite direction to the primary beam and are collected by an on-axis annular detector with a pinhole in the center. The detector is located between the objective aperture and the top deflector. When the signal electrons arrive at the detector they interact with the *p-i-n* junction of the semiconductor detectors and generate electron-hole pairs. The current from the separation of these electron-hole pairs are amplified and converted into digital signal by an analog-to-digital converter.

The adoption of an on-axis annular detector with a pinhole in the center allows the primary beam and signal electrons to share the same passage. The on-axis detector avoids an introduction of a Wien filter into the column, which separates the signal electrons from the primary beam and bends them toward an off-axis detector. Theoretically for the primary beam the magnetic field force $e\mathbf{V}\times\mathbf{B}$ and electrostatic field force $e\mathbf{E}$ have opposite directions and cancel each other in the Wien filter. But practically it is impossible to match

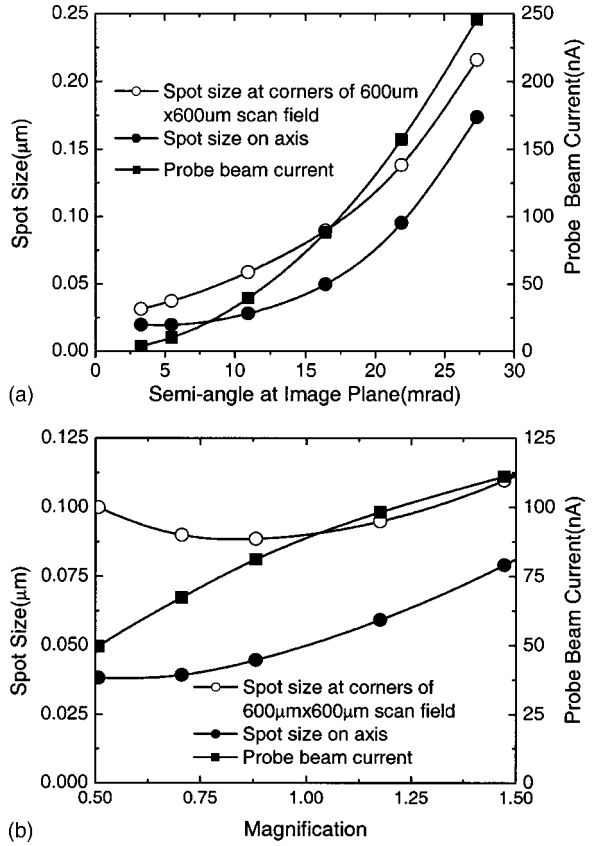

FIG. 2. Beam spot size and probe beam current at the image plane plotted as a function of the image convergent semiangle in (a) (magnification is 1×), and as a function of system magnification in (b). Beam landing energy is 1 keV.

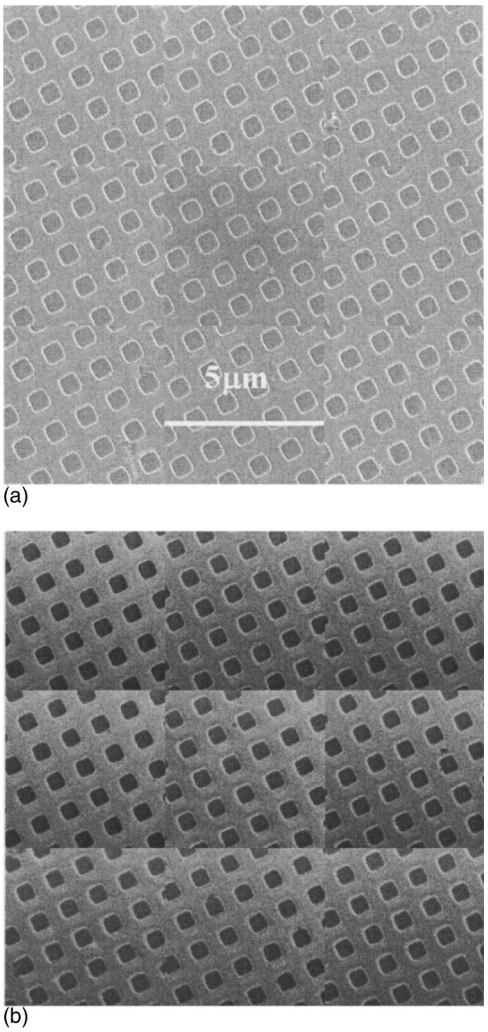

FIG. 3. SEM images of HMI test wafer. Nine 5 μm×5 μm images are taken from four corners, four middle edges and center of a 600 μm ×600 μm large scan field and displayed together. Landing energy is 1 keV in (a) and 300 eV in (b). Probe beam current is 60 nA.

the magnetic force and the electrostatic force in the whole Wien filter region, especially at the fringe region of the deflection fields. So additional aberrations will inevitably be introduced, and affect the achievable resolution. The introduction of a Wien filter also creates difficulties in the column alignment. The on-axis detector makes column alignment much simpler. No electrical alignment is needed in the SORIL column.

The annular detector also offers high signal collection efficiency over a large scan field. Although some on-axis signal electrons have the possibility of passing through the pinhole and thus not be detected, trajectory simulation of secondary and backscattered electrons shows 90% collection efficiency is achievable at the scanning center, because the pinhole of the on-axis annular detector in the SORIL is fabricated to be small, and the detector is placed at a plane where the signal electrons have the largest lateral profile.

An additional benefit of the annular detector is backscattered electron imaging. Secondary electrons can be suppressed back to the specimen by applying a negative bias to the in-lens deflector with respect to the specimen. In that case only the backscattered electron image is obtained.

IV. RESULTS AND DISCUSSION

A. Simulation results

The electron optical properties of the SORIL column are simulated with Munro's Electron Beam Software package.[13] First the field distributions of the compound objective lens and the electrostatic deflectors of the SORIL column are calculated; then the strength ratio and angular relationship of the five deflectors are optimized, with the main field deflectors fulfilling the SOIL condition. The simulated beam spot size, both on axis and at corners of the 600 μm×600 μm scan field, is plotted as a function of convergent semiangle at the image plane in Fig. 2(a). All geometrical and chromatic aberrations are included. The Gaussian image magnification is 1× and the landing energy is 1 keV. The energy spread of 1 eV and the source size of 15 nm are used in the simulation. In Fig. 2(b) the beam spot size is plotted as a function of the Gaussian image magnification when the aperture size remains unchanged. The change of the magnification is achieved by adjusting the condenser lens voltage. In both

Figs. 2(a) and 2(b), the calculated beam probe current obtained at the specimen surface is also shown, assuming an electron gun angular intensity of 1 mA/srad. Figure 2(b) shows that the increase in magnification can greatly boost the beam probe current without seriously degrading the resolution at corners of the large scan field. Our simulation result also shows that the beam landing angle is less than 0.4° with respect to the normal direction of the specimen surface at the corners of the 600 μm $\times$ 600 μm scan field. This allows the bottom of high aspect ratio trenches or holes of the wafer pattern to be observed over the entire scan area.

B. Experimental results

The SORIL column has been constructed and installed onto HMI's e-beam wafer inspection tool, eScan™ 300. The system performances, including resolution and distortion, were tested against the simulated results. A standard silicon sample with an array of square patterns is used to check the distortion of the large scan field. It is found that the distortion at corners and edges of the 600 μm $\times$ 600 μm scan field is less than 0.3 μm. In Fig. 3, two images of HMI standard test wafer are shown, one taken with a landing energy of 1 keV, the other with 300 eV. The probe beam current for both images is 60 nA. From the images, it is apparent that the resolution on the axis and at the corners of the 600 μm $\times$ 600 μm scan field is very uniform.

V. CONCLUSION

A SORIL column is designed and constructed.[14] Duodecapole electrostatic deflectors are innovatively employed to fulfill the mixed-field SOIL condition. A scan field of 600 μm $\times$ 600 μm is achieved with spot size less than 0.1 μm and beam landing angle less than 0.4°. An on-axis annular semiconductor detector with a pinhole at the center is utilized to collect signal electrons. Backscattered electron image can be obtained conveniently by suppressing secondary electrons. The SORIL's capabilities of the large scan field, high resolution and wide range of low landing energy enables eScan™ 300 to be a powerful electron beam wafer inspection and in-line process-monitoring tool.

ACKNOWLEDGMENTS

Many people at HMI contributed mechanics, electronics, and software for the SORIL column. The authors wish to recognize the special contributions from Chung-Shih Pan, Jack Jau, and Yi-Xiang Wang.

[1]W. D. Meisburger, J. Vac. Sci. Technol. B **10**, 2804 (1992).
[2]H. Ohiwa, E. Goto, and A. Omo, Electron. Commun. Jpn. **54B**, 44 (1971).
[3]H. C. Pfeiffer and G. O. Langner, J. Vac. Sci. Technol. **19**, 1058 (1981).
[4]Z. W. Chen, P. Y. Qiu, and J. K. Wang, Optik (Stuttgart) **64**, 341 (1983).
[5]M. A. Sturans, P. F. Petric, H. C. Pfeiffer, W. Stickel, and M. S. Gordon, J. Vac. Sci. Technol. B **8**, 1682 (1990).
[6]Z. W. Chen, G. A. C. Jones, and H. Ahmed, J. Vac. Sci. Technol. B **6**, 2009 (1988).
[7]Y. Zhao and A. Khursheed, Optik (Stuttgart) **110**, 563 (1999).
[8]Y. Zhao and A. Khursheed, J. Vac. Sci. Technol. B **17**, 2795 (1999).
[9]Y. W. Yau, R. F. W. Pease, A. A. Iranmanesh, and K. J. Polasko, J. Vac. Sci. Technol. **19**, 1048 (1981).
[10]T.-T. Tang and J.-P. Song, Optik (Stuttgart) **84**, 108 (1990).
[11]C. H. Schaefer, J. Vac. Sci. Technol. B **4**, 1237 (1986).
[12]T. Goto, S. Konon, T. Someya, K. Tanaka, and S. Miyuachi, J. Vac. Sci. Technol. B **1**, 1289 (1983).
[13]X. Zhu and E. Munro, J. Vac. Sci. Technol. B **7**, 1862 (1989).
[14]Z. W. Chen, U.S. Patent No. 6,392,231 (21 May 2002).